INFECTION AND IMMUNITY, Dec. 1997, p. 5088–5095 Vol. 65, No. 12
0019-9567/97/$04.00+0

Escherichia coli Cytolethal Distending Toxin Blocks the HeLa Cell Cycle at the G_2/M Transition by Preventing cdc2 Protein Kinase Dephosphorylation and Activation

CHRYSTEL COMAYRAS,[1] CHRISTIAN TASCA,[1] SYLVIE YVONNE PÉRÈS,[1] BERNARD DUCOMMUN,[2] ERIC OSWALD,[1] AND JEAN DE RYCKE[1]*

Unité Associée de Microbiologie Moléculaire, Institut National de la Recherche Agronomique et Ecole Nationale Vétérinaire,[1] and Institut de Pharmacologie et de Biologie Structurale, Centre National de la Recherche Scientifique,[2] Toulouse, France

Received 3 July 1997/Returned for modification 5 September 1997/Accepted 19 September 1997

Cytolethal distending toxins (CDT) constitute an emerging heterogeneous family of bacterial toxins whose common biological property is to inhibit the proliferation of cells in culture by blocking their cycle at G_2/M phase. In this study, we investigated the molecular mechanisms underlying the block caused by CDT from *Escherichia coli* on synchronized HeLa cell cultures. To this end, we studied specifically the behavior of the two subunits of the complex that determines entry into mitosis, i.e., cyclin B1, the regulatory unit, and cdc2 protein kinase, the catalytic unit. We thus demonstrate that CDT causes cell accumulation in G_2 and not in M, that it does not slow the progression of cells through S phase, and that it does not affect the normal increase of cyclin B1 from late S to G_2. On the other hand, we show that CDT inhibits the kinase activity of cdc2 by preventing its dephosphorylation, an event which, in normal cells, triggers mitosis. This inhibitory activity was demonstrated for the three partially related CDTs so far described for *E. coli*. Moreover, we provide evidence that cells exposed to CDT during G_2 and M phases are blocked only at the subsequent G_2 phase. This observation means that the toxin triggers a mechanism of cell arrest that is initiated in S phase and therefore possibly related to the DNA damage checkpoint system.

Cytolethal distending toxins (CDT) constitute an emerging toxin family whose members have been found in several unrelated bacterial species of medical interest, including *Escherichia coli* (12, 23, 24, 30), *Shigella dysenteriae* (19), *Campylobacter* sp. (18, 25), and *Haemophilus ducreyi* (3). In all cases, the genetic structure encoding CDT activity included three adjacent or slightly overlapping chromosomal genes (called *cdtA*, *cdtB*, and *cdtC*) encoding proteins with similar molecular masses (27, 29, and 20 kDa, respectively). In *E. coli*, CDT genes were characterized in two enteropathogenic strains (24, 30), where they are chromosomally encoded, and, in a necrotoxigenic strain also producing cytotoxic necrotizing factor 2, where they are plasmid encoded (23). However, the percentage of identity of the predicted proteins is highly variable and shows the heterogeneity of CDT, even within *E. coli* species.

CDT was originally defined by its ability to induce giant elongated cells in CHO tissue cultures upon prolonged incubation (12). The biological activity exerted by CDT on cell cultures has been more precisely defined on the HeLa epithelial cell line (23). The three types of CDT from *E. coli* described above were all shown to inhibit cell division, causing an irreversible block at the G_2/M stage of the cell cycle. This mitotic block leads to cell death only 3 to 5 days after exposure to the toxin, a period of time during which cells continue to synthesize proteins and to grow, becoming up to 10-fold larger than control cells (23). Inhibition of eukaryotic cell division through specific blocking in G_2/M phase of the cell cycle constitutes an original mode of action for a bacterial toxin. Interestingly, this activity bears some resemblance with that exerted by such unrelated agents as the Vpr protein of human immunodeficiency virus type 1 (28, 29) and several DNA-damaging agents, which also cause a block in G_2/M phase of the HeLa cell cycle (15).

Cyclin-dependent kinases in association with their cyclin regulatory units regulate progression through the cell cycle. A complex between the cdc2 (cdk1) protein kinase and cyclin B has been shown to control entry into mitosis in every eukaryotic species (5, 17). The cellular concentration and distribution of cyclin B1 and the state of activation of cdc2 are known to be critical determinants of the transition from G_2 to mitosis (11, 17). In normal cells, cyclin B1 accumulates in the cytoplasm of interphase cells and enters the nucleus only at the beginning of mitosis, before nuclear lamina breakdown (27). cdc2 is expressed at a constant level over the different phases of the cell cycle, but its tyrosine phosphorylation status increases during interphase to reach a maximum level in late G_2. Mitosis is then initiated by cdc25-phosphatase-dependent dephosphorylation of cdc2, an event which fully activates cdc2 kinase (4, 17). In the present study, we sought first to define more precisely the stage at which the HeLa cell cycle was blocked by CDT and second to determine the molecular mechanism underlying this block. To this end, we have monitored on synchronized HeLa cells the early events that occur between cell exposure to the toxin and imposition of the G_2/M block. We have shown that CDT blocks the cell cycle in G_2, and not in M, and that it prevents the dephosphorylation-dependent activation of the cdc2-cyclin B complex. Moreover, we provide evidence that the G_2 block induced by CDT is triggered through pathways that are similar to those utilized by DNA-damaging agents.

* Corresponding author. Mailing address: Unité Associée INRA/ENVT de Microbiologie Moléculaire, Ecole Nationale Vétérinaire, 23 Chemin des Capelles, 31076 Toulouse Cedex, France. Phone: 33 5 61 19 38 85. Fax: 33 5 61 19 39 75.

MATERIALS AND METHODS

CDT preparation and determination of cytotoxic endpoint. CDT-I was produced from *E. coli* DH5α hosting recombinant plasmid pDS7.96, which contains

the three open reading frames (*cdtA*, *cdtB*, and *cdtC*) necessary to encode CDT activity (30). This strain was kindly provided by James Kaper, Center for Vaccine Development, University of Maryland. The toxic preparation consisted in the sterile supernatant of a 24-h Trypticase soy broth aerated culture. The control preparation consisted of the supernatant of *E. coli* DH5α hosting the same cloning plasmid (pUC19) without insert. CDT-II and CDT-III preparations were produced as sterile sonicated lysates from *E. coli* DH5α containing recombinant plasmid pCP2123 (24) (kindly provided by Carol Pickett, Chandler Medical Center, University of Kentucky) and recombinant plasmid pEOFH10 (23), from our laboratory, respectively. The toxic and control preparations were aliquoted and kept at −20°C.

For each preparation, the 95% cytotoxic dose (CD_{95}) was defined as the highest dilution which, following a 1-h application on HeLa cell cultures, gave at least 95% elongated cells after 72 h of incubation (23). Unless otherwise specified, 2 CD_{95} was used in all experiments described below. The control preparation (from DH5α hosting pUC19) did not display any significant decrease in cell growth or any morphological alteration compared to untreated cells. In the text, "control cells" refers to cells exposed to the control preparation.

Cell synchronization and flow cytometry analysis of DNA and cyclin B1 contents. HeLa cells (ATCC CCL2) were grown at 37°C in Eagle minimal essential medium with Earle's salt, L-glutamine (200 mM), and 10% fetal calf serum in a 5% CO_2 atmosphere. Synchronization at the G_1/S border was performed on nonconfluent cell cultures (about 10^6 for a 10-cm-diameter culture dish) by the double thymidine block (DTB) method (31), and synchronization in mitosis (prometaphase) was performed by culture in the presence of nocodazole (100 nM) for 16 h as described previously (31).

For the analysis of DNA content by flow cytometry, cells were trypsinized, washed in phosphate-buffered saline (PBS) and then fixed in 1% formaldehyde in PBS (pH 7.4) for 15 min on ice. Then, after three washes in PBS, they were suspended in 70% ice-cold ethanol and immediately kept at −20°C for at least 2 h. After fixation, cells (about 10^6) were rehydrated in PBS for 30 min at room temperature, permeabilized by 0.1% Triton X-100 in PBS (pH 7.4), and incubated at 4°C for 30 min in the dark in 1 ml of PBS containing propidium iodide (PI; 10 μg/ml; Sigma) and RNase (1 mg/ml; Sigma).

For the combined analysis of both cyclin B1 and DNA in flow cytometry (8), cells (about 10^6) were trypsinized, fixed, and kept in 70% ethanol as described above. After rehydration in PBS, they were permeabilized with 0.25% Triton X-100 for 5 min on ice and incubated overnight at 4°C in the presence of the mouse monoclonal antibody GNS-1 (Pharmingen) diluted 1:100 in PBS containing 1% bovine serum albumin (BSA). Cells were then washed and incubated for 1 h with fluorescein isothiocyanate (FITC)-conjugated goat anti-mouse immunoglobulin G (IgG) antibody (Sigma) diluted 1:40 in PBS containing 1% BSA. The cells were washed again, resuspended in 1 ml of PBS containing PI (10 μg/ml; Sigma) and RNase (1 mg/ml; Sigma), and incubated for 30 min at room temperature in the dark.

Flow cytometry analysis was performed on a FACScalibur flow cytometer (Becton Dickinson), using the red (PI) emission (630 nm) for DNA quantification and green (FITC) emission (530 nm) for cyclin B1 quantification. The data from 10^4 cells were collected and analyzed by using CellQuest software (Becton Dickinson).

Fluorescence microscopy. HeLa cells were cultivated in eight-well Lab-Tek tissue culture chamber slides (Nunc). At specified times, they were washed with PBS and fixed with absolute methanol at −20°C for 6 min. After drying, cells were rehydrated in PBS containing 1% BSA and incubated overnight at 4°C in the presence of a 1:100 dilution in PBS (containing 1% BSA) of one the following monoclonal antibodies: mouse BF683 (Pharmingen) for cyclin A, mouse GNS-1 (Pharmingen) for cyclin B1, or rat YL1/2 (Sera-lab) for α-tubulin. After three washes in PBS, cells were incubated for 1 h in the presence of FITC-conjugated goat anti-mouse IgG antibody (Sigma) or rabbit anti-rat IgG antibody (Vector), diluted 1:40 in PBS containing 1% BSA. After a further step of DNA staining with diaminophenylindole (DAPI; 0.1 μg/ml) in the case of microtubule staining and three more washes in PBS, slides were mounted in Vectashield mounting medium (Vector) and examined by fluorescence microscopy (Leica DMRB fluorescence microscope), using a 40× fluorescence immersion objective lens.

cdc2 purification from cell lysates. After cultivation in the conditions specified in Results, HeLa cells were trypsinized and then washed in Earle balanced salt solution (Gibco). The cell pellet was lysed in an Eppendorf tube for 15 min on ice in a 50 mM Tris-HCl buffer (pH 7.4) containing Triton X-100 (0.1%), NaCl (150 mM), $MgCl_2$ (10 mM), EDTA (5 mM), NaF (50 mM), dithiothreitol (1 mM), glycerophosphate (50 mM), orthovanadate (0.1 mM), and protease inhibitor cocktail (complete; Boehringer, Mannheim, Germany). The lysate was then centrifuged at 4°C (15,000 rpm, 10 min) to eliminate the insoluble fraction, and the protein content of the supernatant was determined by the Bio-Rad protein assay.

cdc2 was then purified from lysates by using a commercial product consisting of recombinant yeast $p13^{suc1}$ covalently bound by CNBr to agarose (Upstate Biotechnology). Lysates (2 mg of total protein for Western blot analysis and 200 μg for kinase activity) were reconstituted in lysis buffer in a final volume of 1 ml, to which 25 μl of p13-agarose beads was added. After 2 h of incubation with agitation at 4°C, beads were pelleted by centrifugation and washed twice in the lysis buffer before kinase assay or Western blot analysis.

Histone H1 kinase assay. The ability of purified cdc2 from cell lysates to phosphorylate histone H1 was assessed as previously described (7). Pellets of purified cdc2 complexed to p13-agarose conjugate, prepared as described above, were suspended in 40 μl of a reaction mix containing Tris-HCl (100 mM; pH 7.4), $MgCl_2$ (10 mM), dithiothreitol (1 mM), ATP (100 μM; Sigma), calf thymus histone H1 (400 μg/ml; Boehringer), and [γ-^{32}P]ATP (125 μCi/ml; Amersham) and incubated for 30 min in a 30°C water bath. After incubation, beads were eliminated by centrifugation and 8-μl aliquots of the supernatant were pipetted onto 1- by 1-cm pieces of P81 ion-exchange paper (Whatman), which specifically retains histone H1. Four aliquots, including a negative control for the calculation of background radioactivity, were tested for each experimental point. Papers were immersed in tap water containing 150 mM H_3PO_4, with five changes of water. After a final rinsing in ethanol and drying, pieces of paper were transferred to scintillation vials to which scintillation fluid (Aquasafe 500; Zinsser Analytic) was added. Radioactivity was determined by liquid scintillation counting. The kinase activity of each lysate was defined as the mean counts per minute minus mean background value.

Western blot analysis of cdc2. cdc2 bound to p13-agarose conjugates, prepared as described above, was extracted with 40 μl of sodium dodecyl sulfate (SDS)-polyacrylamide gel electrophoresis (PAGE) sample buffer, and run in SDS-PAGE (12% gel), using color wide-range molecular weight markers (Sigma). Proteins were blotted onto Immobilon-P membrane (Millipore) filters, using 10 mM cyclohexylamino-1-propanesulfonic acid buffer (Research Organics) containing 10% methanol. The membrane was cut between markers of 29 and 45 kDa and blocked by Superblock blocking buffer (Pierce) containing orthovanadate (0.5 mM). In the first step, the membrane was then incubated overnight at 4°C with antiphosphotyrosine monoclonal antibody clone 4G10 (Upstate Biotechnology) diluted 1:1,000 in PBS containing 0.1% Tween 20, 5% goat serum, and 0.5 mM orthovanadate, followed, after three washes in PBS, by secondary goat anti-mouse IgG (Fab specific)-peroxidase conjugate diluted 1:5,000 as described above (Sigma). The blot was developed by using the ECL chemiluminescence detection system (Amersham). In the second step, the membrane was stripped in 70 mM Tris-HCl (pH 6.8) containing 2% SDS and 100 mM 2-mercaptoethanol, blocked as described above, and reprobed overnight with rabbit anti-cdc2 kinase peptide antibody against the carboxyl terminus (Gibco) diluted 1:500 as described above, followed by secondary goat anti-rabbit IgG-peroxidase conjugate (Biosys) diluted 1:800. The blot was developed as described above.

RESULTS

The G_2/M block caused by CDT is not dependent on cell cycle status at time of exposure. We first checked if the susceptibility of HeLa cells to CDT was dependent on position in the cell cycle. Cells synchronized at G_1/S by the DTB method, in S phase (4 h after release from DTB) and in G_2 phase (8 h after release from DTB), and in M phase by nocodazole were exposed for 1 h to the CDT-I or to the control preparation. Cell cycle distribution was then analyzed by flow cytometry analysis of DNA content 24 h after the exposure period (Fig. 1). When exposed to CDT, the large majority of cells accumulated in G_2/M, irrespective of their position in the cell cycle at the time of exposure. In contrast, control cells analyzed at the same time displayed a clearly different pattern, returning to an almost asynchronized normal distribution 24 h after G_2 and M exposure.

In the same way, no significant difference was observed in the overall sensitivity of cells to CDT according to their position in the cell cycle, as shown by a dose-response study in microtiter plates. The estimated CD_{95} was not significantly different from that observed with unsynchronized cells (i.e., it corresponded to a 1/1,280 dilution of the culture supernatant).

Cells exposed to CDT during G_2 and M phases are arrested at the subsequent G_2/M phase. The data displayed in Fig. 1 indicate that cells exposed to CDT at the G_1/S border or in S phase were arrested in the same cycle, since they could not have reached the next G_2/M phase within a 24 h period of time. This is in agreement with the known durations of the phases of HeLa cell cycle, which are about 7 h for G_1, 8 h for S, 4 h for G_2, and 1 h for M (31). However, it was not possible from the data displayed in Fig. 1 to determine whether cells exposed in G_2 and M phases were arrested during the same cycle or during the subsequent one, since they could well have reached

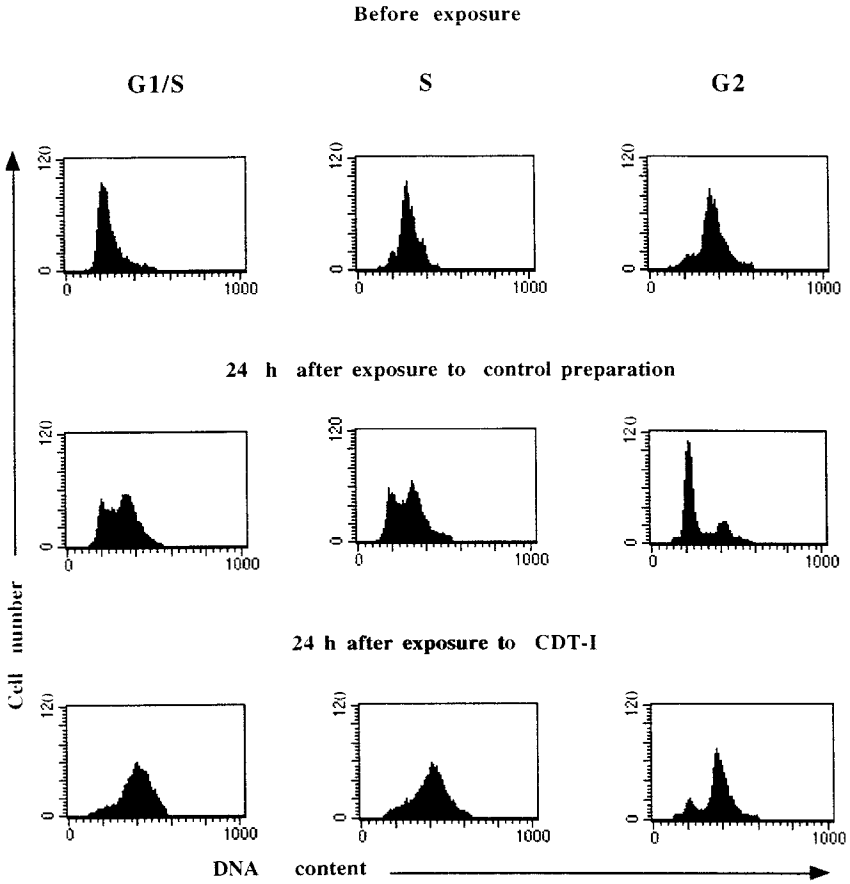

FIG. 1. Induction of G_2/M block by CDT in synchronized HeLa cells exposed in G_1/S, S, and G_2. HeLa cells were synchronized at the G_1/S border by the DTB method. They were exposed for 1 h to CDT-I or the control preparation at time of release (G_1/S), 4 h later (S), or 8 h later (G_2). Cell distribution according to DNA content was analyzed just before exposure or 24 h later by flow cytometry after staining of DNA with PI. About 10,000 cells were analyzed per sample. In each case, the G_1 peak was arbitrarily centered at channel 200. In all cases, cells exposed to the toxin were blocked in G_2/M 24 h after exposure.

a new G_2/M phase after a 24-h period of time. To elucidate this matter, we exposed cells synchronized in G_2 to the toxin for 1 h and studied their DNA distribution after shorter times of incubation after exposure (15, 18, and 24 h). As shown in Fig. 2, 15 h after exposure in G_2, a large majority of cells had initiated a new cycle, and they were blocked in G_2/M only after 24 h of incubation. These results show that most of the cells exposed in G_2 were not blocked in the same cycle but that they had to go through a S phase to be arrested at the subsequent G_2/M transition. The same observation was made with cells synchronized in mitosis by nocodazole (not shown). In addition, it may be relevant that although the large majority of cells exposed in G_2 were arrested in G_2/M, a minority (approximately 15%) were arrested in G_1 (Fig. 1 and 2).

CDT does not affect progression through S phase. The foregoing results did not indicate whether progression through S phase was slowed by the toxin, as is the case, for example, with some DNA-damaging agents also causing a G_2/M block (15). To elucidate this point, we exposed the synchronized cells to the toxin or the control preparation for 1 h at the G_1/S border and analyzed their DNA content by flow cytometry 8 h later. As shown in Fig. 3, the progression of CDT-exposed cells through S phase did not differ significantly from that of control cells, since 50 and 59% of cells, respectively, were estimated to be positioned in the G_2 peak at that time.

Cyclin B1 increase is not affected by CDT during G_2 progression, but cells are blocked before prophase initiation. As shown by fluorescence microscopy after staining of cellular DNA with DAPI, no figure of mitosis, including early prophase with characteristic chromatin condensation and reorganization of microtubules into mitotic spindle, was observable in cells arrested by CDT 24 h after exposure (Fig. 4). This observation suggested that cells accumulated before initiation of prophase. To corroborate this hypothesis, we monitored the expression of cyclin A and cyclin B1 during progression of cells toward the block. As shown previously, these two cyclins are considered relevant indicators of progression through G_2 and M phases since their level increases progressively from late S to M phase. In normal cells, cyclin A is degraded during mitosis just prior to metaphase, whereas degradation of cyclin B1 occurs later, at the transition between metaphase and anaphase (8, 27). The concentration and distribution of cyclins A and B1 in unsynchronized control cells and in cells blocked by CDT (24 h after exposure) were first examined by immunofluorescence microscopy (Fig. 5). In asynchronized control cells, the intensity and cellular distribution of cyclins A and B1 were dependent on position in the cell cycle. Cyclin A was located exclusively in the nucleus, and its intensity increased up to prophase (Fig. 5A). The highest concentration of cyclin B1 was observed in the nucleus during prophase and metaphase. In interphase cells, cyclin B1 remained located in the perinuclear area and was readily perceptible only in late G_2 in our experimental conditions (Fig. 5C). In cells blocked by CDT, 24 h after exposure the intensity and distribution of both cyclin A and

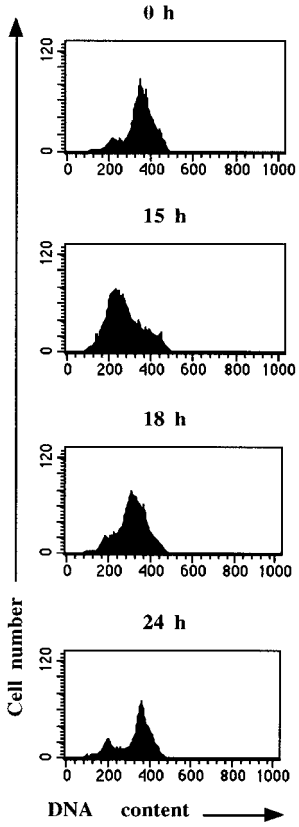

FIG. 2. Demonstration that most of the cells exposed to CDT during G_2 phase of the cell cycle were arrested only at the subsequent G_2 phase. HeLa cells were synchronized in G_2 by the DTB method followed by 8 h of incubation. They were then exposed to CDT-I or the control preparation for 1 h. Cell cycle progression was assessed by flow cytometry quantification of PI-stained DNA at 15, 18, and 24 h after exposure to the toxin. About 10,000 cells (4,000 at 24 h) were analyzed per sample. In each case, the G_1 peak was arbitrarily centered at channel 200.

cyclin B1 were highly homogeneous among cells. Cyclin A clearly accumulated in the nucleus, without reaching the level of intensity observed with control cells in prophase (Fig. 5B). Cyclin B1 also accumulated in the perinuclear area up to the level of late G_2 control cells, without translocating in the nucleus (Fig. 5D). These observations confirm that at least in the early phases of the block, cells did not proceed past the G_2 stage.

Cyclin B1 expression was then monitored quantitatively by flow cytometry in synchronized cells after release from G_1/S block followed by 1 h of exposure to the toxin or the control preparation (Fig. 6). In control cells, the pattern of cyclin B1 expression was in accordance with previous observations (8), i.e., a steady increase from end of S phase up to 11 h, a time that corresponds approximately to entry in mitosis. In CDT-treated cells, which were blocked in G_2, the average level of cyclin B1 was not significantly different from that of control cells up to 11 h. However, at 11 h, the increase in cyclin B1 was not stopped in CDT-treated cells, in contrast to control cells ($P < 0.05$). The continued increase of cyclin B1 in CDT-treated cells in the long term was confirmed in assays using unsynchronized cells (Fig. 7). We observed that the average content of cyclin B1 in cells exposed to CDT increased by a factor 2.1 (163/77) from 4 to 16 h after exposure and a factor 3.6 (280/77) from 4 to 48 h after exposure. The quantitative determination of cyclin B1 by flow cytometry analysis confirmed that CDT-treated cells were arrested in late G_2 (and not in M) and showed that the toxin did not interfere with the regular increase of cyclin B1 during cycle progression to G_2 or with its continued synthesis after establishment of the G_2 block itself. This result further suggested that cyclin B1, the regulatory subunit of the mitosis promoting complex, was not itself directly affected by the toxin and thus prompted us to investigate a possible modification of cdc2, the catalytic subunit of this complex.

The cdc2 protein kinase is inactivated by CDT. We compared the kinase activity and state of phosphorylation of cdc2 in control and CDT-exposed asynchronous cells 24 h after exposure. Cells arrested in prometaphase by nocodazole were used as a positive control. To extend the validity of our results, we performed this experiment on the three partially related types of *E. coli* CDT so far described (23, 24, 30). As shown in Fig. 8, cells blocked in G_2 by all three CDTs displayed a low level of kinase activity, not significantly different from that of control cells in interphase and roughly 8 to 10% of the activity of nocodazole-treated cells. The phosphorylation status of cdc2 in the same samples was studied by Western blot analysis after affinity purification using $p13^{suc-1}$-agarose conjugate (Fig. 8). Using antiphosphotyrosine antibodies and, after stripping of the blotting membrane, anti-cdc2 antibodies, we demonstrated the existence of the three isoforms of cdc2, with a clear concentration of the slow-migrating, highly phosphorylated form of cdc2 in cells exposed to the three CDTs and blocked in G_2. In the normal, asynchronous population of cells exposed to the control preparation, the lack of kinase activity was associated, as expected, with an overall low level of tyrosine phosphorylation and with a higher concentration of the lower fast-migrating band. In nocodazole-treated cells arrested in prometaphase, the lower isoform was dominant, and, interestingly, the intermediate band appeared to be also slightly tyrosine phosphorylated. We presume that this reflected the presence of a dephosphorylation intermediate that is phosphorylated on both tyrosine 15 and threonine 161 but not on threonine 14 (2). Altogether, these observations led us to the conclusion that CDT blocks the cell cycle progression at the

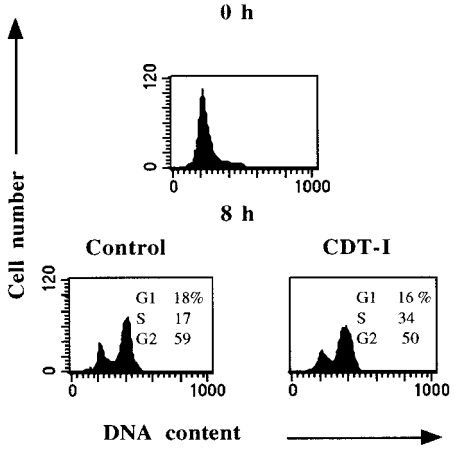

FIG. 3. Progression of synchronized HeLa cells from G_1/S through S phase following exposure to CDT. HeLa cells were synchronized at the G_1/S border by the DTB method. At the time of release from G_1/S, they were exposed for 1 h to CDT-I or to the control preparation. Eight hours later, a time which corresponds roughly to the end of S phase, DNA content was analyzed by flow cytometry after PI staining. About 10,000 cells were analyzed per sample. In each case, the G_1 peak was arbitrarily centered at channel 200. S phase was not significantly slowed by CDT compared to the control preparation.

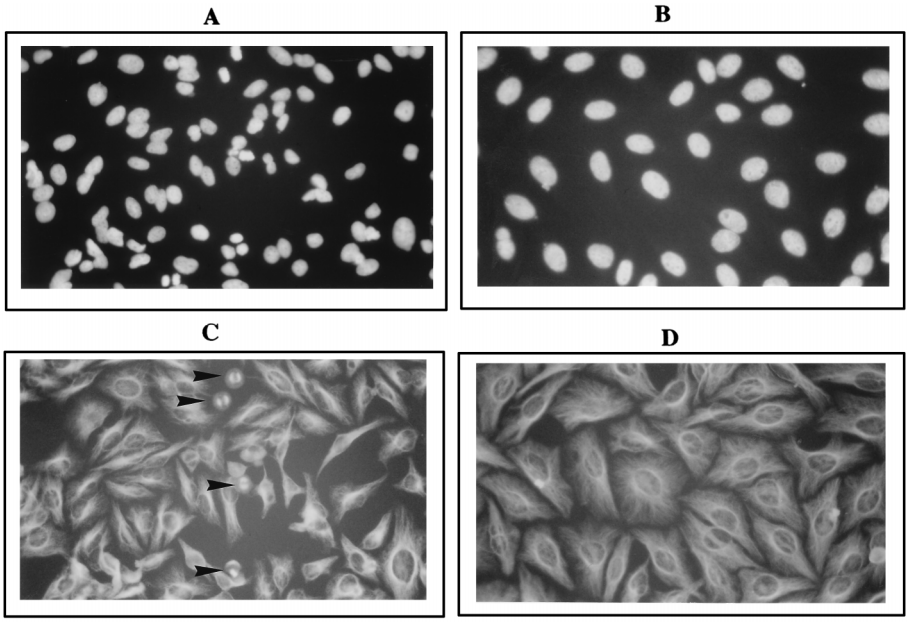

FIG. 4. Fluorescence microscopy of cells exposed for 1 h to CDT-I (B and D [same field]) or the control preparation (A and C [same field]) 24 h after exposure. (A and C) DAPI staining; (C and D) microtubule staining. Note the absence of mitotic figures and the increased nuclear size in CDT-treated cells compared to control cells, where several figures of mitosis are visible (arrowheads).

G_2/M transition by preventing cdc2 protein kinase dephosphorylation and subsequent activation.

DISCUSSION

In this study, we investigated the early events that follow exposure of HeLa cells to *E. coli* CDT, in an attempt to clarify the mechanisms that lead to the G_2/M block reported previously (23). We have demonstrated (i) that cells accumulate in late G_2 (and not M), (ii) that the G_2-phase block is associated with stabilization of the hyperphosphorylated form of the cdc2 protein kinase, and (iii) that the toxin interferes with a cellular mechanism that is triggered in S phase.

Our demonstration that cells accumulated in G_2, and not in

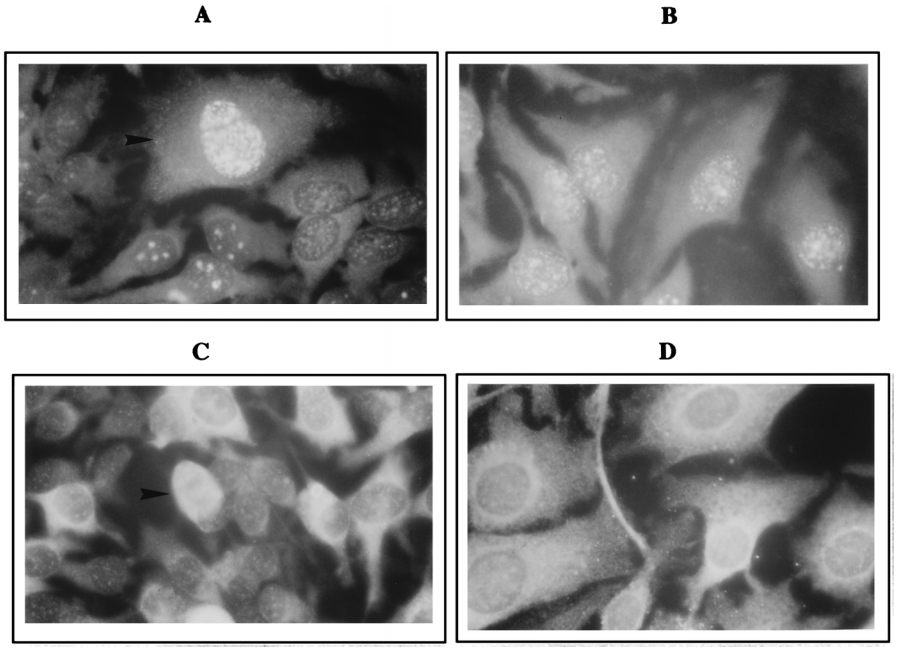

FIG. 5. Fluorescence microscopy of cyclin A (A and B) and cyclin B1 (C and D) distribution in asynchronous control cells (A and C) and CDT-I-treated cells (B and D) 24 h after exposure. Cyclins were stained by indirect immunofluorescence using FITC-conjugated antibodies as the secondary reagent. Note in particular that in CDT-treated cells, the distribution and intensity of both cyclin A (nuclear) and cyclin B1 (perinuclear) are highly homogeneous, indicating a block in late G_2. By contrast, cyclin contents of control cells are highly heterogeneous (mitotic cells are indicated by arrowheads).

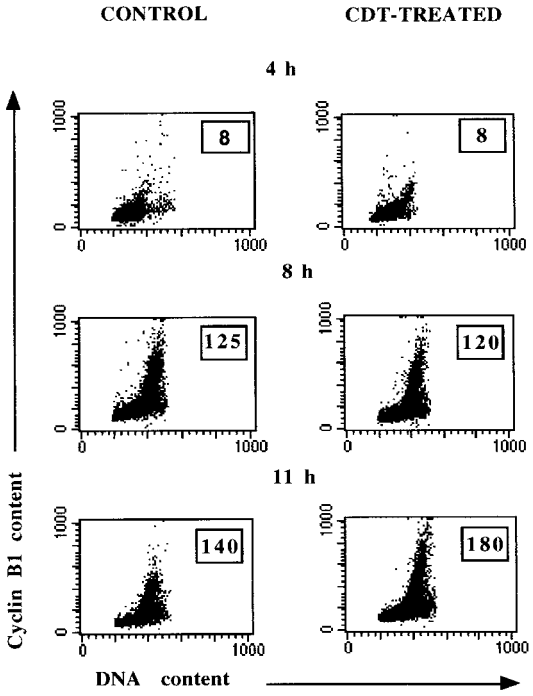

FIG. 6. Expression of cyclin B1 in synchronized HeLa cells after exposure to CDT or to the control preparation, determined by flow cytometry analysis. HeLa cells were synchronized in G_1/S by the DTB method. At release from the G_1/S block, they were exposed for 1 h to CDT-I or to the control preparation. They were analyzed for cyclin B1 and DNA contents 4 h (S phase), 8 h (G_2), or 11 h (M) later. Cyclin B1 was stained by indirect immunofluorescence using FITC-conjugated antibody as the secondary reagent and stained for DNA with PI. Relative cyclin B1 content according to DNA content was determined by bivariate flow cytometry analysis. About 10,000 cells were analyzed per sample. The average level of cyclin B1 content of the total population (arbitrary units), as determined by CellQuest statistical software, appears in the upper right corner of each analysis. Note that the cyclin B1 increase through S and G_2 was not significantly different in control cells and in CDT-treated cells up to 11 h ($P > 0.05$). After 11 h, cyclin B1 continued to increase in CDT-treated cells, while it started to decline significantly in control cells ($P < 0.05$), which progressed into G_1 phase.

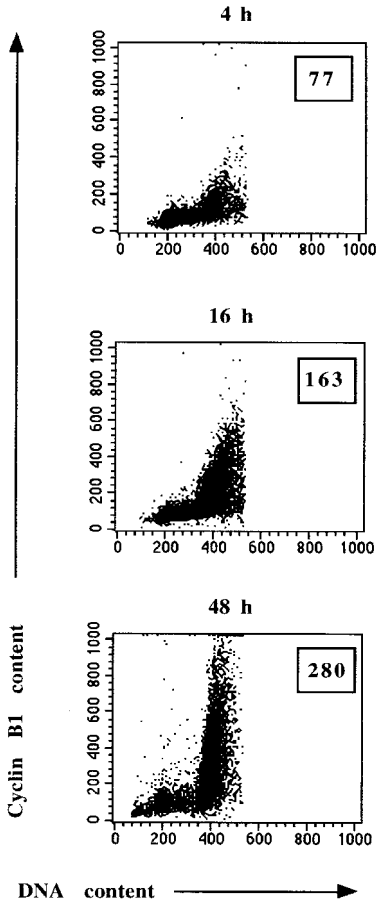

FIG. 7. Expression of cyclin B1 in unsynchronized HeLa cells after exposure to CDT or to the control preparation, determined by flow cytometry analysis. HeLa cells were exposed for 1 h to CDT-I or to the control preparation. They were analyzed for cyclin B1 and DNA contents 4 h, 16 h (G_2), or 48 h later. Cyclin B1 was stained by indirect immunofluorescence using FITC-conjugated antibody as the secondary reagent and stained for DNA with PI. Relative cyclin B1 content according to DNA content was determined by bivariate flow cytometry analysis. About 10,000 cells were analyzed per sample. The average level of cyclin B1 content of the total population (arbitrary units), as determined by CellQuest statistical software, appears in the upper right corner of each analysis. Note that in CDT-treated cells, which were blocked in G_2 phase, cyclin B1 increased steadily up to at least 48 h after exposure.

M, is based primarily on the fact that blocked cells did not display in fluorescence microscopy any mitotic figures 24 h after exposure, using DNA- and microtubule-specific staining. More specifically, we observed no early condensation of chromatin or any significant reorganization of microtubules into a mitotic spindle in these cells (Fig. 4). This observation was confirmed by fluorescence microscopy of cyclin A and cyclin B1, whose localization and concentration indicate that cells were arrested in late G_2. We reported previously that this block was irreversible and that cell death of blocked cells started from about 72 h after exposure (23). The description of the delayed events that precede cell death and analysis of its biological determinism will be the subject of a future study.

To approach the determinism of the G_2 block caused by CDT, we monitored the behavior of the cdc2 protein kinase and of cyclin B1, its regulatory unit (17). We first demonstrated by flow cytometry analysis that cyclin B1 expression was not significantly affected in synchronous cells exposed in G_1/S compared to synchronous control cells (Fig. 6). During S and G_2 progression, cyclin B1 accumulated in exposed cells at approximately the same rate as in control cells, in accordance with previously described pattern (8). However, the overall level of cyclin B1 continued to increase significantly at least up to 48 h after exposure (Fig. 7) while, as expected (8), it dropped in control cells at entry into mitosis. These data demonstrate that the block cannot be accounted for by a lack of cyclin B1 expression.

The role of cdc2 was assessed by using two complementary approaches: quantification of its kinase activity and molecular analysis of its phosphorylation status in SDS-PAGE immunoblotting. Our results show that 24 h after exposure, blocked cells had a low level of cdc2 kinase activity, which was associated with the stabilization of the hyperphosphorylated slow-migrating form of the molecule (Fig. 8). Since dephosphorylation of cdc2 on Tyr-15 and Thr-14 residues is a prerequisite for its activation and for entry into mitosis, and since cyclin B1, its regulatory subunit, was apparently not affected in CDT-exposed cells, we can reasonably infer from our results that the absence of cdc2 dephosphorylation is the immediate event that accounts for the G_2 block. More generally, CDT would interfere, directly or indirectly, on a transduction pathway that determines the state of phosphorylation of cdc2. In other words, CDT may act directly on the phosphorylation/dephosphorylation machinery that regulates the activation of cdc2 at

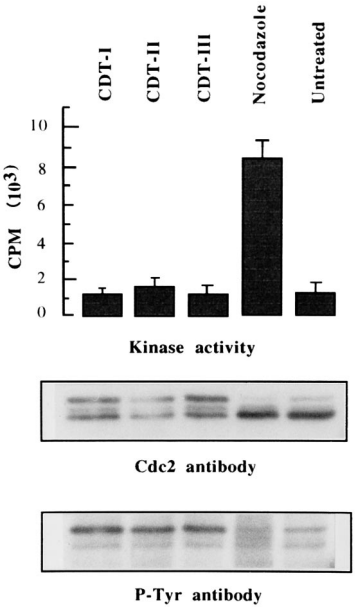

FIG. 8. Histone H1 kinase activity and state of phosphorylation of p34^{cdc2} in cells exposed to *E. coli* CDT. Asynchronized HeLa cells were exposed for 1 h to 2 CD_{95} of each of the three CDT preparations (see Materials and Methods) and processed for analysis 24 h after exposure. Two controls were included: (i) asynchronized cells 24 h after a 1-h exposure to the control negative preparation and (ii) cells blocked in prometaphase by a 16-h exposure to nocodazole. cdc2 present in cell lysates (200 μg of total protein for kinase activity and 2 mg for immunoblot analysis) was purified by affinity on Sepharose-bound p13. Kinase activity in precipitates was assessed by the level of [γ-^{32}P]ATP incorporation by histone H1 as measured by liquid scintillation counting (four determinations per sample). Average numbers of counts per minute (minus background radioactivity) and standard errors are shown. The state of phosphorylation of cdc2 was assessed by immunoblotting on a same membrane, first by probing with a monoclonal antibody against phosphotyrosine (P-Tyr) and then, after stripping of the membrane, by reprobing with a polyclonal antibody against the carboxyl terminus of cdc2. The kinase activity of CDT-treated cells was inhibited almost to the level of asynchronous control cells in interphase. In CDT-cells blocked in G_2, this inhibition was associated with hyperphosphorylation of the upper slow-migrating form of cdc2.

mitosis or, alternatively, may impair cdc2 activation by inducing the effect of a cyclin-dependent kinase inhibitor. In that case, change in the phosphorylation status of cdc2 would be only indirect and would reflect the cell cycle arrest prior to the dephosphorylation event. Two immediately upstream molecular determinants of cdc2 phosphorylation are known at the present time (5, 17). The first one is the cdc25 phosphatase, which, upon activation, removes the inhibitory phosphate from Thr-14 and Tyr-15 residues of cdc2. The second, antagonistic to the first one, is the mammalian equivalent for yeast Wee1-like tyrosine kinase, which phosphorylates cdc2 on Tyr-15 (9, 21). The possibility that one or the other of these effectors is involved should be tested.

A further clue to the determinism of the G_2 block caused by CDT is provided by our demonstration that in contrast to cells exposed in G_1/S and S, most cells exposed in G_2 and M are blocked not at the current cycle but at the next one (Fig. 2). This important observation means that passage through S phase is required for the G_2 block to be triggered. This would imply that the toxin interferes with a transduction cascade that is initiated in S phase, i.e., during DNA replication. Such a cascade could be the so-called DNA damage checkpoint, which is the mechanism that detects damaged DNA and generates a signal that arrests cells in the G_1 phase of the cell cycle, slows down S phase, arrests cells in the G_2 phase, and induces the transcription of repair genes (6, 22). Two hypotheses can be raised: either CDT is able to induce DNA damage, for example, through acting on enzymes of the replication machinery, or it interferes with early downstream components of the DNA damage checkpoint system. In mammalian cells, only the G_1 damage checkpoint is understood with some detail (6). It is controlled by at least three genes, called *ATM*, *p53*, and *p21*. p53 protein activates transcription of p21, a tight-binding inhibitor of the cyclin-dependent kinases that controls entry into S phase. Much less is known regarding the determinism of the G_2 damage DNA checkpoint in mammalian cells (6, 22). In the present study, HeLa cells accumulated most exclusively in G_2 and insignificantly in G_1 (except when cells were exposed in G_2), and the rate of their progression through S phase was not affected, at least at the dose tested. These peculiarities are not in contradiction with the potential involvement of the DNA damage checkpoint, since expression of p53 and p21 is known to be repressed in HeLa cells (10). In these conditions, activation of the DNA damage checkpoint in HeLa cells inevitably results in a predominant G_2 block due to lack of cdc2 activation, as already demonstrated in this cell line with such different DNA-damaging agents as camptothecin, etoposide, nitrogen mustard (13–15), and ionizing radiations (1, 16). Another consequence of our observation that a 1-h exposure to CDT during G_2-phase-induced blocking at the subsequent cell cycle is that toxin activity is maintained through a complete cell cycle, i.e., at least 20 h, in spite of its absence from the culture medium. This conclusion is corroborated by the fact that the overall sensitivity of cells exposed in G_2 was not significantly different from that of cells synchronized in G_1/S or in S.

The inhibitory activity of CDT on cdc2 protein kinase activation has been demonstrated in the present study with the three *E. coli* CDT types cloned so far (23, 24, 30). Moreover, this property seems to apply as well to CDT from other bacterial species, since CDT from *Campylobacter jejuni* also appears to block cell cycle in G_2 through inactivation of cdc2 (26). Although the effect of CDT in cultured cells is novel for a bacterial toxin, it bears striking similarities with that of a recently discovered viral protein: the Vpr of human immunodeficiency virus type 1 (29). Vpr also causes a G_2 block due to inhibition of p34^{cdc2} in different cell lines, including HeLa cells (29), through pathways that are similar to those used by DNA-damaging agents. The relevance of the cell cycle inhibitory effect of CDT in in vivo pathogenesis now remains to be explored. The fact that different variants of this toxin are found in unrelated bacterial species such as *S. dysenteriae* (19, 20), *Campylobacter* sp. (18, 25), and *H. ducreyi* (3) would indicate that the in vivo biological function conferred by this factor gives a highly selective advantage to its hosts. All of the pathogens mentioned above are pathogenic for epithelia, either the intestinal epithelium (for *E. coli*, *S. dysenteriae*, and *Campylobacter* sp.) or the vaginal epithelium (for *H. ducreyi*). The pathogenic role of CDT in diarrheal diseases is substantiated by the recent observation that CDT from *S. dysenteriae* is able to induce tissue damage and fluid accumulation in the descending colon of orally infected suckling mice (20). The relation between this in vivo effect and the inhibition of cell division that we have investigated in the present study should now be examined. One can speculate that the toxin is able to inhibit the growth of actively dividing crypt cells, thus preventing the rapid renewal of the epithelium and leading to the intestinal lesions.

ACKNOWLEDGMENTS

We thank Alain Milon for constant support in the course of this study and for helpful comments and critical reading of the manuscript.

We are also indebted to James Kaper and Carol Pickett for the gifts of plasmids pDS7.96 and pCP2123, respectively.

This work was supported in part by grant 1335 from the European Community Program FAIR and grant 9507783 from the Conseil Régional de la Région Midi-Pyrénées. S.Y.P. is a recipient of a scholarship from the Ministère de l'Enseignement Supérieur et de la Recherche.

REFERENCES

1. **Barth, H., I. Hoffmann, and V. Kinzel.** 1996. Radiation with 1Gy prevents the activation of the mitotic inducers mitosis-promoting factor (MPF) and cdc25-C in HeLa cells. Cancer Res. **56:**2268–2272.
2. **Borgne, A., and L. Meijer.** 1996. Sequential dephosphorylation of $p34^{cdc2}$ on Thr-14 and Tyr-15 at the prophase-metaphase transition. J. Biol. Chem. **271:**27847–27854.
3. **Cope, L. D., S. Lumbley, J. L. Latimer, J. Klesney-Tait, M. K. Stevens, L. S. Johnson, M. Purven, R. S. Munson, Jr., T. Lagergard, J. D. Radolf, and E. J. Hansen.** 1997. A diffusible cytotoxin of *Haemophilus ducreyi*. Proc. Natl. Acad. Sci. USA **94:**4056–4061.
4. **Draetta, G., and D. Beach.** 1988. Activation of cdc2 protein kinase during mitosis in human cells: cell cycle-dependent phosphorylation and subunit rearrangement. Cell **54:**17–26.
5. **Dunphy, W. G.** 1994. The decision to enter mitosis. Trends Cell Biol. **4:**202–207.
6. **Elledge, S. J.** 1996. Cell cycle checkpoints: preventing an identity crisis. Science **274:**1664–1672.
7. **Félix, M. A., P. R. Clarke, J. Coleman, F. Verde, and E. Karsenti.** 1993. *Xenopus* egg extracts as a system for studying mitosis, p. 253–283. *In* P. Fantes, and R. Brooks (ed.), The cell cycle: a practical approach. IRL Press, Oxford, England.
8. **Gong, J., F. Traganos, and Z. Darzynkiewicz.** 1995. Discrimination of G2 and mitotic cells by flow cytometry based on different expression of cyclins A and B1. Exp. Cell Res. **220:**226–231.
9. **Heald, R., M. McLoughlin, and F. McKeon.** 1993. Human Wee1 maintains mitotic timing by protecting the nucleus from cytoplasmically activated cdc2 kinase. Cell **74:**463–474.
10. **Hwang, E. S., L. K. Naeger, and F. DiMaio.** 1996. Activation of the endogenous p53 growth inhibitory pathway in HeLa cervical carcinoma cells by expression of the bovine papillomavirus E2 gene. Oncogene **12:**795–803.
11. **Jackson, P. K.** 1996. Cell cycle: cull and destroy. Curr. Biol. **6:**1209–1212.
12. **Johnson, W. M., and H. Lior.** 1988. A new heat-labile cytolethal distending toxin produced by *Campylobacter* spp. Microb. Pathog. **4:**115–126.
13. **Lock, R. B., F. Galperina, R. C. Feldhoff, and L. J. Rhodes.** 1994. Concentration-dependent differences in the mechanisms by which caffeine potentiates etoposide cytotoxicity in HeLa cells. Cancer Res. **54:**4933–4939.
14. **Lock, R. B., and P. K. Killing.** 1993. Responses of HeLa and Chinese hamster ovary cdc2/cyclin-B kinase in relation to cell cycle perturbations induced by etoposide. Int. J. Oncol. **3:**33–42.
15. **Maity, A., A. Hwang, A. Janss, P. Philips, W. J. McKenna, and W. G. Muschel.** 1996. Delayed cyclin B1 expression during the G2 arrest following DNA damage. Oncogene **13:**1647–1657.
16. **Metting, N. F., and J. B. Little.** 1995. Transient failure to dephosphorylate cdc2-cyclin B1 complex accompanies radiation-induced G2 phase arrest in HeLa cells. Radiat. Res. **143:**286–292.
17. **Norbury, C., and P. Nurse.** 1992. Animal cell cycles and their control. Annu. Rev. Biochem. **61:**441–470.
18. **Ohya, T., K. Tominaga, and K. Nakazawa.** 1993. Production of cytolethal distending toxin (CLDT) by *Campylobacter fetus* subsp. *fetus* isolated from calves. J. Vet. Med. Sci. **55:**507–509.
19. **Okuda, J., H. Kurazono, and Y. Takeda.** 1995. Distribution of the cytolethal distending toxin A gene (*cdtA*) among species of *Shigella* and *Vibrio*, and cloning and sequencing of the *cdt* gene from *Shigella dysenteriae*. Microb. Pathog. **18:**167–172.
20. **Okuda, J., M. Fukumoto, Y. Takeda, and M. Nishibuchi.** 1997. Examination of diarrheagenicity of cytolethal distending toxin: suckling mouse response to the products of the *cdtABC* genes of *Shigella dysenteriae*. Infect. Immun. **65:**428–433.
21. **Parker, L. L., P. J. Sylvestre, M. J. Byrnes III, F. Liu, and H. Piwnica-Worns.** 1995. Identification of a 95-kDa WEE1-like tyrosine kinase in Hela cells. Proc. Natl. Acad. Sci. USA **92:**9638–9642.
22. **Paulovitch, A. G., D. P. Toczyski, and L. H. Hartwell.** 1997. When checkpoints fail. Cell **88:**315–321.
23. **Pérès, S. Y., O. Marchès, F. Daigle, J. P. Nougayrède, F. Hérault, C. Tasca, J. De Rycke, and E. Oswald.** 1997. A new cytolethal distending toxin (CDT) from *Escherichia coli* producing CNF2 blocks Hela cell division in G2/M phase. Mol. Microbiol. **24:**1095–1107.
24. **Pickett, C. L., D. L. Cottle, E. C. Pesci, and G. Bikah.** 1994. Cloning, sequencing, and expression of the *Escherichia coli* cytolethal distending toxin genes. Infect. Immun. **62:**1046–1051.
25. **Pickett, C. L., E. C. Pesci, D. L. Cottle, G. Russell, A. N. Erdem, and H. Zeytin.** 1996. Prevalence of cytolethal distending toxin production in *Campylobacter jejuni* and relatedness of *Campylobacter* sp. *cdt* genes. Infect. Immun. **64:**2070–2078.
26. **Pickett, C. L.** 1997. Cytolethal distending toxin causes a G2 phase cell cycle block, abstr. B-259, p. 73. *In* Abstracts of the 97th General Meeting of the American Society for Microbiology 1997. American Society for Microbiology, Washington, D.C.
27. **Pines, J., and T. Hunter.** 1991. Human cyclins A and B1 are differentially located in the cell and undergo cell-cycle-dependent nuclear transport. J. Cell Biol. **115:**1–17.
28. **Planelles, V., J. B. M. Jowett, Q. X. Li, Y. Xie, B. Hahn, and I. S. Y. Chen.** 1996. Vpr-induced cell cycle arrest is conserved among primate lentiviruses. J. Virol. **70:**2516–2524.
29. **Poon, B., J. B. M. Jowett, S. A. Stewart, R. W. Armstrong, G. M. Rishton, and I. S. Y. Chen.** 1997. Human immunodeficiency virus type 1 *vpr* gene induces phenotypic effects similar to those of the DNA alkylating agent, nitrogen mustard. J. Virol. **71:**3961–3971.
30. **Scott, D. A., and J. B. Kaper.** 1994. Cloning and sequencing of the genes encoding *Escherichia coli* cytolethal distending toxin. Infect. Immun. **62:**244–251.
31. **Stein, G., and J. L. Stein.** 1990. Cell synchronization, p. 133–137. *In* R. I. Frishney (ed.), Cell growth and division, a practical approach. IRL Press, Oxford, England.
32. **Tsao, Y., P. D'Arpa, and L. F. Liu.** 1992. The involvement of active DNA synthesis in camptothecin-induced G2 arrest: altered regulation of cdc2/cyclin B. Cancer Res. **52:**1823–1829.

Editor: J. T. Barbieri